Numerical Error Analysis for Deterministic Kinetic Solutions of Low-Speed Flows

Alina A. Alexeenko

School of Aeronautics and Astronautics, Purdue University, West Lafayette, IN 47907.

Abstract. The computational cost of the direct simulation Monte Carlo solutions of rarefied flows increases with decreasing average flow velocity due to larger noise-to-signal ratio and a longer time to reach the steady state. For such low-speed flows, the discrete-ordinate solution of kinetic model equations can provide accurate and computationally efficient numerical modeling. In this work, analysis of the numerical errors of discrete-ordinate solution of the kinetic model equation is carried out using the Richardson extrapolation on non-uniform meshes. The procedure is illustrated for a second-order finite-difference solution of ellipsoidal statistical kinetic model equation for a two-dimensional low-speed rarefied flow generated by a non-uniformly heated plate.

INTRODUCTION

Starting from the pioneering work by Bird in early 1960s[1] on the development of stochastic numerical methods for kinetic description of gas flows, the direct simulation Monte Carlo (DSMC) method has evolved into a powerful numerical tool that has provided accurate and efficient solutions to many important problems of rarefied gas dynamics.[2, 3] However, the computational cost of the DSMC method increases with decreasing Mach number due to: (a) explicit time integration in the DSMC algorithm and, therefore, long time to reach a steady-state; (b) larger sample sizes to attain a required signal-to-noise ratio when the average gas velocity is small in comparison to thermal speed[4]. Additionally, coordinate transformation in physical space domain that could have greatly increased computational efficiency for a high-aspect ratio geometries can not be implemented in an atomistic simulation. Last but not least, there are inherent difficulties in coupling a stochastic method for gas flow modeling with conventional deterministic simulations of solid material response for the integrated system analysis including coupled thermal-fluid-structural interactions. The aforementioned computational issues stimulate applications of deterministic kinetic methods for numerical modeling of low-speed microscale flows.

APPLICATION OF KINETIC MODELS FOR LOW-SPEED FLOWS

For modeling of low-speed microscale flows we consider the solution of the steady-state Boltzmann equation with a simplified collision operator. The two-dimensional single-collision time approximation of the Boltzmann equation has the form:

$$U\frac{\partial f}{\partial x}+V\frac{\partial f}{\partial y}=\nu(f_0-f) \tag{1}$$

where $f=f(x,y,U,V,W)$ is the distribution function, x and y are Cartesian coordinates, U,V, and W are velocity components, and ν is the collision frequency. For the Bhatnagar-Gross-Krook (BGK) model $f_0=f_M=n(2\pi RT)^{-3/2}exp(-\frac{\vec{C}^2}{2RT})$ is the local equilibrium Maxwell distribution. For the ellipsoidal statistical (ES) model[5] $f_0=f_G$ is the local isotropic three-dimensional Gaussian

$$f_G=\frac{n}{\sqrt{(2\pi)^3\det[\lambda_{ij}]}}\exp(-\varepsilon_{ij}c_ic_j),\qquad \lambda_{ij}=(\frac{1}{Pr})RT\delta_{ij}+\frac{1-1/Pr}{\rho}p_{ij} \tag{2}$$

where $[\varepsilon] = [\lambda]^{-1}$, $\vec{C} = \vec{U} - \vec{\vec{U}}$ is thermal velocity, p_{ij} is the pressure tensor, and Pr is the Prandtl number. If Prandtl number Pr=1 then $f_G = f_M$ and Eq. (1) gives the original BGK model.

The model kinetic equation Eq. (1) can be solved using a finite-difference method and standard discrete-ordinate procedure[6] for interpolation of the distribution function in the velocity space. Comparison of the DSMC and ES solutions for pressure and temperature-driven[7] microchannel flows and moving microbeam flow[8] showed that the deterministic solution of ES model kinetic equation can provide accurate numerical predictions for low-speed rarefied flows. For low-speed rarefied flows the computational cost of solution of model kinetic equations is reduced an order of magnitude or more compared to DSMC simulations. However, because of the multidimentional phase space, including both physical coordinates and velocities, when solving kinetic model equations, mesh sizes are limited and assessment of numerical errors becomes critical. In this work, Richardson extrapolation is applied for numerical error quantification of the low-speed rarefied flow generated by a non-uniformly heated plate.

RICHARDSON EXTRAPOLATION

If discrete solution $F(h)$ is a continuous and differentiable function of a representative mesh size h, it has a series representation[9]:

$$F(h) = F_{exact} + C_k h^k + O(h^{k+1})$$

where F_{exact} is the exact solution (for mesh size $h = 0$) and k is the order of the numerical method. The idea of Richardson extrapolation is to combine solutions on different meshes to eliminate the leading order error terms. For example, for a mesh with a characteristic mesh size h/r, we have:

$$F(\frac{h}{r}) = F_{exact} + C_k(\frac{h}{r})^k + O(h^{k+1})$$

where r is the mesh refinement factor. Combining the two solutions to eliminate the leading error term, we get Richardson extrapolation for the discrete solution on two different meshes as:

$$RE^k(F(h), F(\frac{h}{r})) = \frac{r^k F(\frac{h}{r}) - F(h)}{r^k - 1} = F_{exact} + O(h^{k+1}). \tag{3}$$

If numerical solutions are obtained for three meshes with characteristic mesh sizes h, $\frac{h}{r_1}$ and $\frac{h}{r_2}$, then two leading error terms can be eliminated as:

$$RE^k(F(h), F(\frac{h}{r_1}), F(\frac{h}{r_2})) = \frac{\alpha_2 RE^k(F(h), F(\frac{h}{r_1})) - \alpha_1 RE^k(F(h), F(\frac{h}{r_2}))}{\alpha_2 - \alpha_1} = F_{exact} + O(h^{k+2}) \tag{4}$$

where $\alpha_i = (r_i(r_i^{k-1} + r_i^{k-2} + ... + 1))^{-1}, \quad i = 1, 2.$

The Richardson extrapolation process for eliminating the highest-order error terms in a discrete solution does not depend on a specific numerical method applied to obtain that solution and, thus, it can be used as a post-processing procedure. Applications of the Richardson extrapolation for analysis of mesh convergence for solution of various fluid flow problems using finite-difference and finite volume CFD methods on structured meshes have been reported in Ref. [10]-[13]. Celik and co-workers[10], [11] applied the Richardson extrapolation for solutions of backward-facing step flow using a commercial CFD code on uniform and non-uniform meshes. Because typical CFD solvers use mixed order schemes for approximation of spatial derivatives and fluxes, they suggested to use Richardson extrapolation to determine an apparent order of the method. Bergstrom and Gebart[12] considered methods for estimation of mesh error for solution of a turbulent draft tube flow problem and used the Richardson extrapolation procedure for calculating the mesh size necessary to achieve a target value of the mesh error. Shyy at al[13], while applying Richardson extrapolation for cavity and backward-facing flows assuming a nominal second order accuracy of the method, concluded that the Richardson extrapolation does not work consistently in typical CFD engineering applications for turbulent flows.

In the following section we evaluate the applicability of Richardson extrapolation for mesh convergence analysis of discrete ordinate solution of ES model kinetic equation for a two-dimensional radiometric flow.

EXAMPLE: RADIOMETRIC FLOW

As an example of Richardson extrapolation for discrete-ordinate solution of the ES model kinetic equation we consider a radiometric flow generated by an non-uniformly heated plate. The flow is called "radiometric" because it is similar to the rarefied gas flow that creates the rotation of the vanes of Crookes' radiometer.[14] A schematics of the flow and the boundary conditions are shown in Fig. 1. The two-dimensional computational domain extends from -0.224 m to 0.224 m in X and Y directions. The heated plate is located at the center of the domain and has a height of 38 mm and a width of 9.24 mm. The right and left sides of the plate have the temperature of 410 K and 450 K, respectively. The outer walls of the domain are at the temperature of 300 K. The chamber is filled with argon gas at the pressure of 2 Pa and the Knudsen number based on the width of the plate is equal to 0.29 at a reference temperature of 300 K. The conditions of the calculations are chosen to match the setup of Radiometric Force Actuation (RFA) experiments being conducted at USC.

The numerical solution of the ellipsoidal statistical model equation for the two-dimensional radiometric flow was obtained using discrete ordinates in the velocity space and a second order finite-difference method in physical coordinate space. In the numerical solutions presented below the Gauss-Hermite half range quadrature [15] of order 8 and three-eighth's rule with 96 ordinates are used for the integration over velocity magnitude and angle, respectively. A second-order finite-difference scheme is used for all interior mesh points with a 5-point stencil chosen to allow explicit calculations of the distribution function ordinates for each velocity quadrant.

The analysis of discretization error of the solution in physical coordinate space was conducted using four non-uniform meshes. The mesh parameters are listed in Table 1. Each mesh for calculations of the radiometric flow consisted of three blocks, with non-uniform mesh points spacing. The power-law mesh point distribution, $\frac{x_{j+1}-x_j}{x_1-x_0} = \beta^j$, was used in both x and y directions with an exponent $\beta = 1.1$. The meshes a and d in the vicinity of the plate are plotted in Fig. 2.

TABLE 1. Mesh parameters.

Designation	Block 1	Block 2	Block 3	Refinement factor, r
a	31 ×46	19 × 31	31 × 46	1
b	41 ×61	25 × 41	41 × 61	$\frac{4}{3}$
c	51 ×76	31 × 51	51 × 76	$\frac{5}{3}$
d	61 ×91	37 × 61	61 × 91	2

Thermal stresses generate the flow between the cold outer walls of the domain and the heated plate and in the direction of the temperature gradient along the edges of the plate. The temperature contours and streamlines calculated using the finest mesh d are shown at the bottom of Fig. 1. Two counter rotating vortices develop in the flow chamber. The temperature flowfields calculated using the four different meshes are nearly identical, whereas the size of the smaller vortex at the cold side of the plate is very sensitive to the mesh resolution. Fig. 3 shows the temperature profiles along the centerline ($Y = 0$) for the four different meshes. The maximum difference in the calculated temperature are at the hot side of the plate and are less than 1 K between the solutions on the coarsest mesh a and the finest mesh d. In the whole flow domain the difference in the temperature calculated using the coarsest and the finest mesh are less than 0.25%.

The velocity flowfields are more sensitive to the mesh size. Fig. 4 shows the X-velocity flowfields in the vicinity of the plate calculated using the coarsest mesh a (top) and the finest mesh d (bottom). The velocity fields are quantitatively different with the maximum difference along the centerline of more than 25% near the hot side of the plate. The Richardson extrapolation Eq. (3) applied to pairs of solutions obtained on different meshes are shown in Fig. 5. The extrapolated velocity values agree very well with a maximum difference along the centerline less than 3%. The other macroparameter that is more sensitive to the mesh resolution in the radiometric flow is the number density. Fig. 8 shows the number density profiles along the centerline for the four different meshes. Richardson extrapolation of the number density using the Eq. (3) and Eq. (4) are plotted in Fig. 9 and 10, respectively. The maximum difference between the density values along the centerline for the finest and the coarsest meshes is 3.4% while that for Richardson extrapolation of Eq. (3) and Eq. (4) is less than 2% and 0.04%, respectively. Thus, Richardson extrapolation does allow to consistently eliminate the leading error terms and to increase the accuracy of the deterministic numerical solutions of kinetic models on non-uniform meshes.

The thermal stress flow at rarefied conditions generates a total force normal to the plate. The value of the total force is

measured in the RFA experiments and can be predicted by the numerical modeling. The quantification of the numerical error in the calculated total force can be carried out using Richardson extrapolation based on Eq. (4) which eliminates two leading error terms. The approximate relative error of the solution obtained using a mesh with the characteristic size h is $\varepsilon = \frac{RE^k - F(h)}{RE^k}$. Table 2 lists the calculated forces and approximate relative error for solutions obtained on different meshes. The force per unit span of the plate in the Z-direction is calculated from the momentum flux on the plate. The span of the plate in experiments is 0.127 m. Equation (4) is used to obtain Richardson extrapolation for the three meshes a,b and c, $R^2(a,b,c)$ which approximates the exact solution for the total force.

TABLE 2. Calculated total force.

Discrete solution	Total force F, μ N	Est. error ε, %
Mesh a	44.905	5.41
Mesh b	45.636	3.87
Mesh c	46.147	2.79
Mesh d	46.364	2.34
RE^2(a,b)	46.576	1.89
RE^2 (a,c)	46.846	1.32
RE^2 (b,d)	46.946	1.11
RE^2(a,b,c)	47.473	–

CONCLUDING REMARKS

Deterministic solution of model kinetic equations, e.g., ellipsoidal statistical model, can provide accurate numerical predictions for low-speed microscale flows at a significantly reduced computational cost compared to the DSMC method. Numerical studies of radiometric flow demonstrated that Richardson extrapolation can be used for numerical error quantification of discrete-ordinate solutions of kinetic equations on uniform and non-uniform meshes.

ACKNOWLEDGMENTS

The work was supported in part by the U.S. Air Force Office of Scientific Research and the Propulsion Directorate of the Air Force Research Laboratory at Edwards Air Force Base, California. The author would like to thank Drs. E. Phillip Muntz, Sergey Gimelshein and Felix Sharipov for useful discussions of kinetic models.

REFERENCES

1. Bird, G.A., *Phys. Fluids*, 1963, 1518-1519.
2. Gimelshein, S.F., and Ivanov, M.S., *Ann. Rev. Fluid Mech.*, Vol. 30, 1998, pp. 469-505.
3. Oran, E.S., Oh, C.K., and Cybyk, B.Z., *Ann. Rev. Fluid Mech.*, Vol. 30, 1998, pp. 403-441.
4. Cai, C., Boyd, I. D., Fan, J., and Candler, G. V., *J. Thermophys. Heat Transf.*, Vol. 14, No. 3, 2000, pp. 368-378.
5. Andries, P., Le Tallec, P., Perlat, J.P., and Perthame, B., *Europ. J. Mech. B, Fluids*, Vol. 19, No. 6, 2000, pp. 813-830.
6. Aoki, K., Kanba, K., and Takata, S., *Phys. Fluids*, Vol. 9, No. 4, 1997, pp. 1144-1161.
7. Alexeenko, A.A., Gimelshein, S.F., Muntz, E.P., Ketsdever, A.D., *Int. J. of Thermal Sciences*, Vol. 45, No. 11, 2006, pp. 1045-1051.
8. Alexeenko, A.A., Muntz, E.P., Gallis, M.A., and Torczynski,J.R., Comparison of Kinetic Models for Gas Damping of Moving Microbeams, *AIAA Paper 2006-3715*.
9. Roache, P. J., *Ann. Rev. Fluid Mech.*, Vol. 29, pp. 123-160, 1997.
10. Celik, I., and Zhang, W.-M., *J. Fluids Engineering, Transactions of the ASME*. Vol. 117, no. 3, pp. 439-435, 1995.
11. Celik, I., and Karatekin, O.,*J. Fluids Engineering, Transactions of the ASME*. Vol. 119, pp. 584-590, 1997.
12. Bergstrom, J., and Gebart, R., *Int. J. Num. Meth. Heat & Fluid Flow*, Vol. 9, No. 4, pp. 472-486, 1999.
13. Shyy, W., Garbey, M., Appukuttan, A., and Wu, J., *Num. Heat Transfer, Part B*, Vol. 41, pp. 139-164, 2002.
14. Wadsworth, D.C., Muntz, E.P., Pham-Van-Diep, G., and Keeley, P., Crookes' radiometer and micromechanical actuators, In *Rarefied Gas Dynamics, Proc. 19th Int. Symp., Oxford 1994*, pp. 708-714.
15. Shizgal, B. A., *J.Comp. Physics*, Vol. 41, 1981, pp. 309-328.

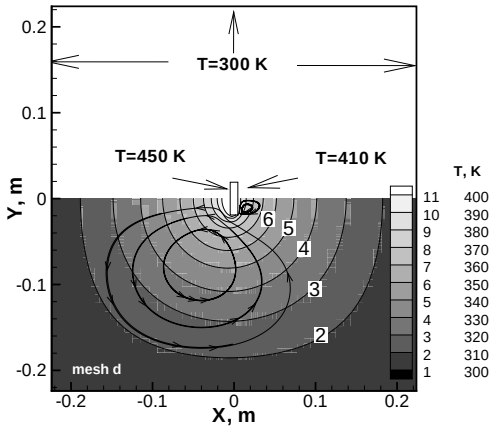

FIGURE 1. Top: Schematic of the computational domain and boundary conditions for radiometric flow. Bottom: Calculated temperature and streamlines for mesh d.

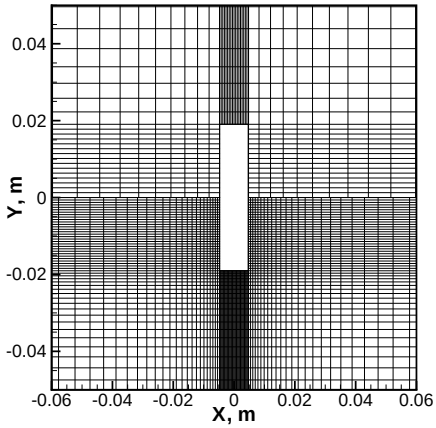

FIGURE 2. Computational mesh in the vicinity of the plate: top - mesh a; bottom - mesh d.

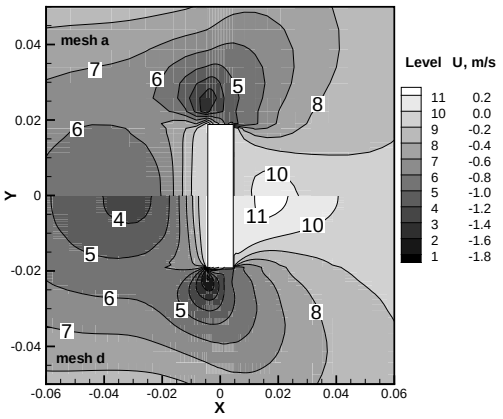

FIGURE 4. X-velocity contours in the vicinity of the plate: top - mesh a; bottom - mesh d.

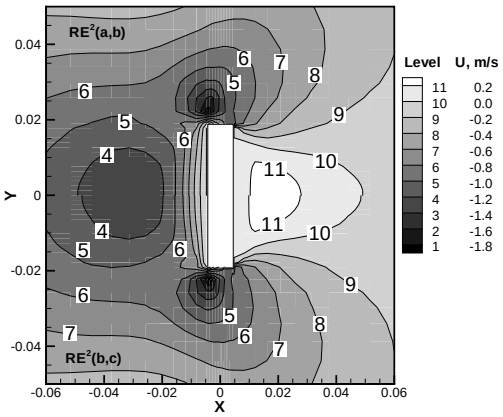

FIGURE 5. Contours of the Richardson extrapolation Eq. (3) for X-velocity in the vicinity of the plate: top - $RE^2(a,b)$; bottom - $RE^2(b,c)$.

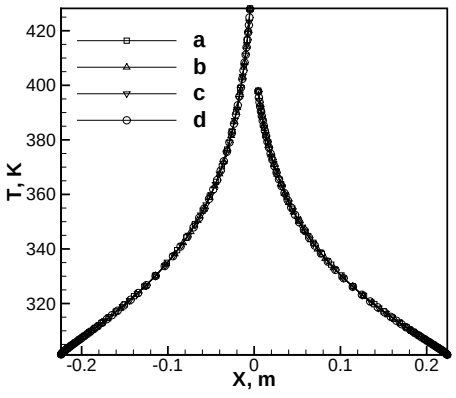

FIGURE 3. Calculated temperature profiles along the centerline for different mesh sizes.

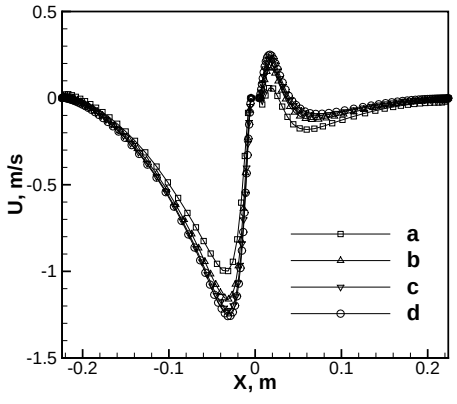

FIGURE 6. Calculated X-velocity profiles for different mesh sizes along the centerline .

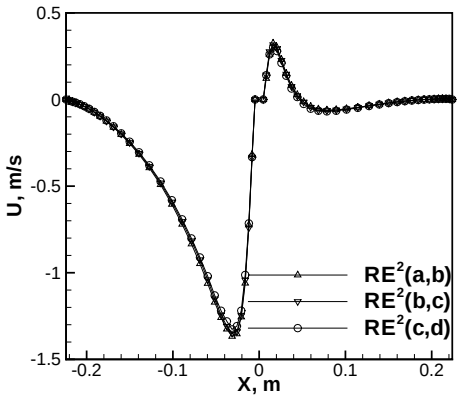

FIGURE 7. Richardson extrapolation Eq. (3) for X-velocity profiles along the centerline.

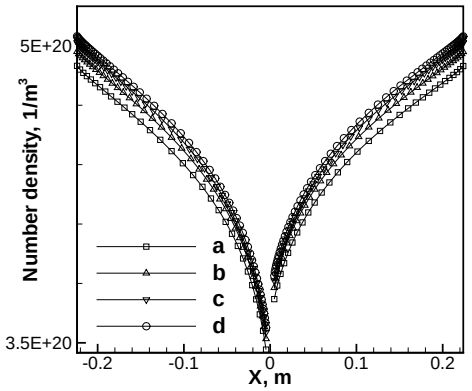

FIGURE 8. Calculated number density profiles for different mesh sizes along the centerline.

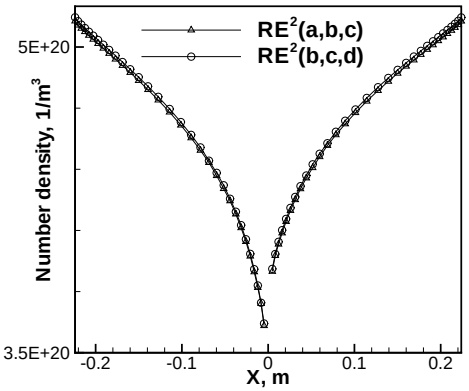

FIGURE 10. Richardson extrapolation Eq. (4) for number density profiles along the centerline.

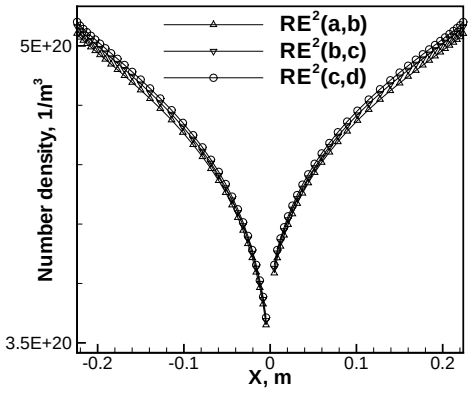

FIGURE 9. Richardson extrapolation Eq. (3) for number density profiles along the centerline.